Electronic Supplementary Material (ESI) for Chemical Communications

Li_4NiTeO_6 as positive electrode for Li-ion batteries

DOI: 10.1039/c3cc46842a

M. Sathiya, K. Ramesha, G. Rousse, D. Foix, D. Gonbeau, K. Guruprakash, A. S. Prakash, M. L. Doublet and J.-M. Tarascon

Supplementary information

Structural Analysis deduced from the refinement of Synchrotron X-Ray diffraction pattern of Li_4NiTeO_6.

The structure of the compound was analyzed by Rietveld refinement against high-resolution synchrotron powder diffraction data, collected on the 11-BM beamline at the Advanced Photon Source (APS, Argonne National Laboratory) with a wavelength of 0.4138Å. Powders were sealed in 1.5 mm diameter kapton capillaries. The 2θ range over which the fit was done is [2°-50°]. We observed some Lorentzian broadening for some reflections (**Figure S1a**), which can arise from size and/or strain effects. Therefore, additional refinements were performed, with the 1/cosθ dependent parameters to fit the intrinsic profile through isotropic size effects, and a tanθ dependence of anisotropic strain. No size broadening was observed and strain parameters, whose S_{hkl} values using Stephens notation[1] are below, led to an improved refinement, as shown on the same set of reflections in **Figure S1b**. The final structural model is shown **Table S1,** and selected bond lengths & bond valence sum analysis were reported in supplementary information-**Table S2.**

1. Stephens, P., Phenomenological model of anisotropic peak broadening in powder diffraction. *Journal of Applied Crystallography* **1999,** 32, (2), 281-289.

Figure S1: Portion of the Synchrotron X-Ray diffraction pattern of Li_4NiTeO_6 (λ=0.4138 Å): a) Rietveld fit with the instrumental resolution function b) adding some anisotropic strain parameters as shown in Table S1.

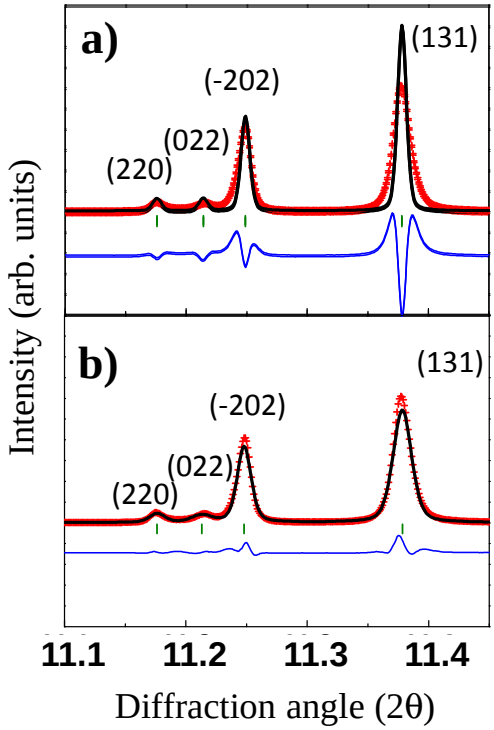

Table S1: Structural parameters of Li_4NiTeO_6 deduced from the Rietveld refinement of Synchrotron XRD.

Space Group	**a (Å)**	**b (Å)**	**c (Å)**	**β (°)**	**Volume (Å^3)**	**Density (g.cm^{-3})**
*C*2/*m*	5.1584(1)	8.8806(1)	5.1366(1)	110.241 (1)	220.777(3)	4.665
Atom	**Wyckoff Site**	**x**	**y**	**z**	**Biso (Å^2)**	**Occupation factor**
Li1	4*h*	0	0.1738(5)	1/2	0.66(6)	1
Li2	2*d*	0	1/2	1/2	0.31(9)	1
Li3/Ni	4*g*	0	0.3335(1)	0	0.43(1)	0.5 Li + 0.5 Ni
Te	2*a*	0	0	0	0.34(1)	1
O1	8*j*	0.2309(2)	0.1533(2)	0.2334(2)	0.29(2)	1
O2	4*i*	0.2302(3)	0	0.7772(3)	0.26(3)	1

Strain Parameters (x10^{-4})								
S_{400}	S_{040}	S_{004}	S_{220}	S_{202}	S_{022}	S_{121}	S_{301}	S_{103}
0.168(2)	0.0083(2)	0.333(3)	0.097(2)	0.162(8)	0.235(2)	0.323(3)	0.195(6)	0.277(7)

Table S2:

Average *M*-O Distances (*M*=Li, Ni, Te), Bond Valence Sum values (BVS) and distortion of octahedra (Δ) obtained from the refinement of the Synchrotron X-Ray diffraction pattern of Li_4NiTeO_6. A bond valence sum analysis with the Zachariasen formula $BVS = e^{(d_0-d)/0.37}$, using d_0 parameters from Brown,[1] was performed and the deduced valences are in perfect agreement with what expected, in particular for Te^{6+} (5.894(9)) for which bond distance to (Te-O) is shorter than the Li/Ni-O ones . Morever, the structural distortion of the MO_6 octahedron (*M*=Li, Ni, Te), has been calculated with the formulae $\Delta = \frac{1}{6}\sum_{n=1}^{6}\left(\frac{(d_n-\langle d\rangle)}{\langle d\rangle}\right)^2$ where, d_n are the individual *M*-O distances and ⟨d⟩ is the average value of the 6 M-O distances. Δ is displayed in the Table and indicates regular octahedra.

Atom	Coordinence	Expected Valence	Average M-O distance (Å)	Distortion Δ ($x10^{-4}$)	BVS
Li1	6	1.000	2.1561(11)	2.923	0.934(3)
Li2	6	1.000	2.1587(5)	24.512	0.959(1)
Li3	6	1.000	2.1047(4)	0.845	1.069(1)
Ni	6	2.000	2.1047(4)	0.845	1.777(2)
Te	6	6.000	1.9236(5)	0.149	5.894(9)
O1	6	-2.000	2.0988(5)	11.793	1.928(3)
O2	6	-2.000	2.1074(7)	24.301	1.928(5)

Reference :

1. I. D. Brown, D. Altermatt, *Acta Crystallographica Section B-Structural Science,* 1985, **41**, 244.

Figure S2:

Schematic representation of the Te inductive effect on the Ni^{2+}/Ni^{4+} redox couple through an orbital interaction viewpoint., i.e. showing the lowering of the redox orbital when Ni^{2+} is surrounded by $3(TeO_6)^{6-}$ octahedra as it occurs in the honeycomb layers of the Li_4NiTeO_3 structure. For sake of clarity only one atomic orbital per element is represented. The global charges added to each molecular entity are required to compensate for the O-excess compared to the solid state stoichiometry. (a) The molecular orbital diagrams of $(Ni^{2+}O_6)^{10-}$ and $(Te^{6+}O_6)^{6-}$ show that Te^{6+} is more covalently bonded to the O^{2-} ligands than Ni^{2+} due to the smaller electronegative difference $\Delta\chi$-Te/O compared to $\Delta\chi$-Ni/O. This leads to a significant energy lowering of the oxygen-like O(π) orbitals in TeO_6 compared to NiO_6. (b) The molecular orbital diagram of the $(Ni^{2+}Te^{6+}{}_3O_{18})^{16-}$ cluster shows that the redox orbital is lowered in energy due to the smaller interaction of Ni^{2+}(3d) orbitals with the strongly electronegative O(π) orbitals of the $(TeO_6)^{6-}$ surrounding octahedra, thus increasing the Ni^{2+}/Ni^{4+} redox potential with respect to Li^+/Li.

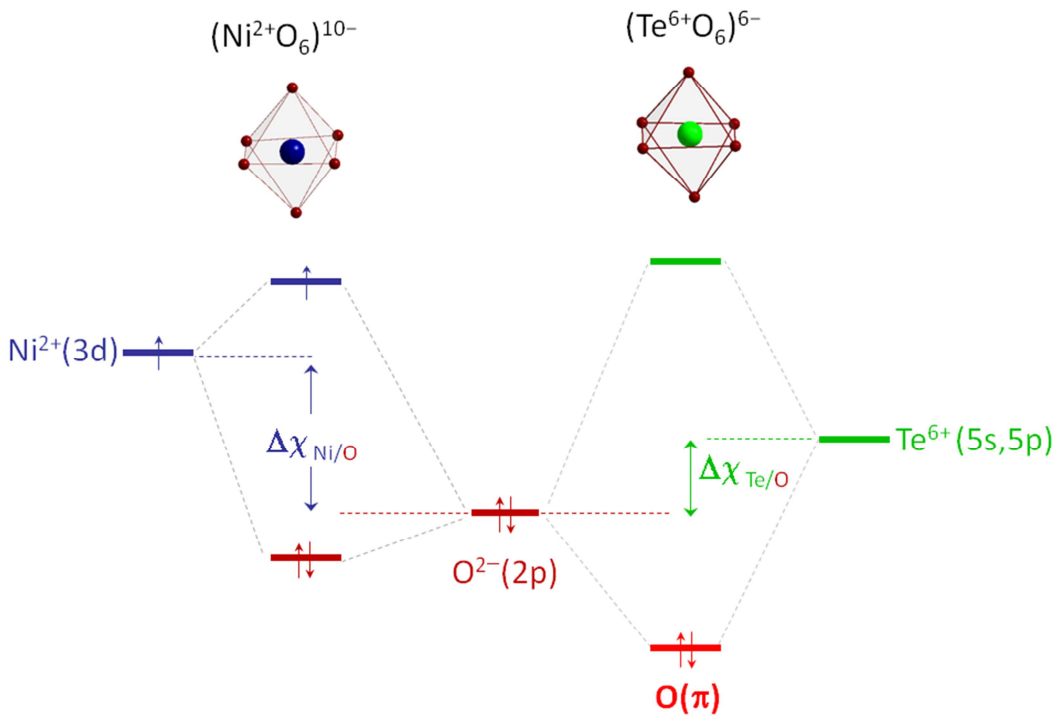
$(Ni^{2+}O_6)^{10-}$
$(Te^{6+}O_6)^{6-}$
$Ni^{2+}(3d)$
$\Delta\chi_{Ni/O}$
$\Delta\chi_{Te/O}$
$Te^{6+}(5s,5p)$
$O^{2-}(2p)$
O(π)

(a)

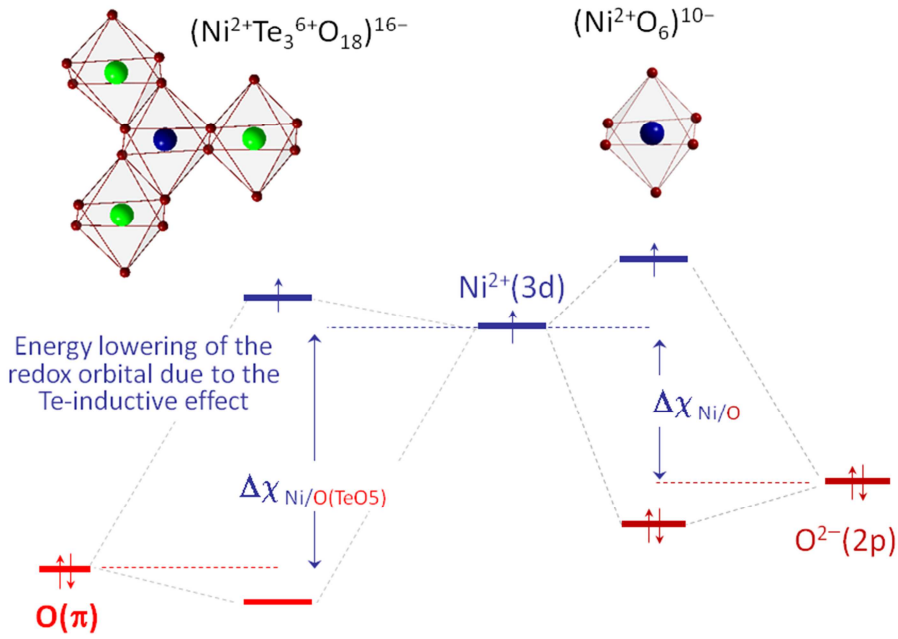
$(Ni^{2+}Te_3{}^{6+}O_{18})^{16-}$
$(Ni^{2+}O_6)^{10-}$
$Ni^{2+}(3d)$
Energy lowering of the redox orbital due to the Te-inductive effect
$\Delta\chi_{Ni/O}$
$\Delta\chi_{Ni/O(TeO5)}$
$O^{2-}(2p)$
O(π)

(b)